

Dynamics of excitable nodes on random graphs

K MANCHANDA*, T UMESHKANTA SINGH and R RAMASWAMY¹

School of Physical Sciences, Jawaharlal Nehru University, New Delhi 110 067, India

¹Present address: University of Hyderabad, Hyderabad 500 046, India

*Corresponding author. E-mail: kaustubh011184@gmail.com

Abstract. We study the interplay of topology and dynamics of excitable nodes on random networks. Comparison is made between systems grown by purely random (Erdős–Rényi) rules and those grown by the Achlioptas process. For a given size, the growth mechanism affects both the thresholds for the emergence of different structural features as well as the level of dynamical activity supported on the network.

Keywords. Excitable nodes; networks; rhythmic activity.

PACS Nos 84.35.+i; 64.60.aq

1. Introduction

Networks of dynamical systems arise in a wide variety of contexts, ranging from neuroscience [1], gene interactions [2], sociology [3], ecology [4] to evolutionary models [5]. The nodes of the network are dynamical systems that interact with one another through coupling, and together with the topological properties of the network, they play a major role in the generation of ‘activity’ in the system.

Understanding the interplay of dynamics and structure on such networks has been a subject of enduring interest [6]. Sustained activity, by which one means the avoidance of eventual fixed point dynamics, usually implies the existence of periodic solutions or the generation of rhythmic processes [7]. Network structure can play a crucial role in this regard [8]: it is well known that topological (connectivity) features have a major impact on a variety of contact process wherein dynamics is important. Examples can be drawn from diverse areas – the spread of epidemics [9,10] or opinions [11], and in communication and information processing [12]. Other contexts where connectivity has a major impact includes the study of synchronization on networks [13] or the generation of complex physiological rhythms [7,13,14].

In our earlier work [15], we have extensively studied the relationship between the topology and dynamics of excitable nodes on Erdős–Rényi (ER) [16] random graphs. Our focus is on rhythmic dynamics, namely periodic solutions, in this representative model. Since the network topology plays an important role, the question of how different growth rules

affect such dynamics is also of interest. For instance, when the graph is grown using preferential attachment [17] to obtain a scale-free network, cycles do not form and therefore rhythmic dynamics is relatively uncommon. In this work, we contrast our earlier results for random networks with those evolved from the Achlioptas growth process [18]. A natural question, given the fact that both networks are random, is whether the growth mechanism affects structural features and thereby alters the dynamics, in particular the thresholds for the emergence of various types of dynamical activity.

This paper is organized as follows. In §2, we briefly discuss the ER and Achlioptas mechanisms and the structural properties of the resulting networks. In §3, the intrinsic dynamics of discrete excitable nodes and the rules of interaction between them are discussed. The interplay between structure and dynamics on these random graphs is described in §4, and a summary is given in §5.

2. Random graphs

We first briefly describe the growth mechanisms for the undirected random graphs being studied here. Consider a graph $\mathcal{G}(n, m)$, where n is the number of nodes and m is the number of edges. A given graph can be characterized by the fraction $f = 2m/n(n-1)$; as $f \rightarrow 1$, the graph becomes fully connected. The adjacency matrix, which is symmetric, contains information on structural properties of the network and is defined in the usual way: if there is a connection between nodes i and j , the element A_{ij} of the adjacency matrix A is 1, else it is 0. In the ER process, the m edges are added at random between pairs of nodes, independently. In the Achlioptas growth process, there is an additional constraint to ensure that the formation of a large cluster is suppressed. At each time step, two random edges m_1 and m_2 are picked independently and a choice between them is made based on the product rule, PR_m , which is as follows [19]:

1. If both edges lead to intercomponent connections, the edge with a lower value of the product of the sizes of the components it merges is selected.
2. If the edge m_1 is intercomponent while the other is intracomponent, then m_2 is chosen since that would not lead to any change in the component size.
3. If both connections are intracomponent, one is chosen at random.

In the present simulations we study graphs with $n = 30$ nodes, and ensemble averages are computed with at least 1000 samples. Shown in figures 1a and c are the proportion of nodes that have an edge (solid curves) for Achlioptas and ER graphs respectively as a function of f . With increasing f the number of isolated nodes decreases (dashed curves). At $f = f_1^a$ and $f = f_1^e$, on an average half the nodes are connected while the other half are isolated in the two graphs, with $f_1^a < f_1^e$. PR_m favours the growth of isolated small clusters, and thus about $n/4$ links are needed to reach 50% connectivity, fewer than for ER graphs.

A cluster is a subset of connected nodes, and the number of clusters of size k is denoted by C_k . Clearly, for $f = 0$, $C_1 = n$ and $C_k = 0$ for $k \neq 1$, while for $f = 1$, $C_n = 1$ and $C_k = 0$ for $k \neq n$. In figures 1b and d, C_2 , C_3 and C_{30} are plotted in both ER and Achlioptas networks. Curve C plots the growth of the total number of clusters normalized by the number of nodes n . The largest cluster C_{30} rises and reaches the plateau of the

C curve at $f = f_2^a$ and $f = f_2^e$ in the two graphs. Henceforth, with an increase in f , every realization of the network leads to the formation of this largest size cluster. As may be expected, there are quantitative differences since PR_m favours the formation of smaller clusters and delays the formation of the fully connected cluster, C_n . Thus $f_2^a > f_2^e$. Since the merging of components is discouraged, this leads to the formation of a larger number of clusters of different sizes and its cumulative effect can be seen on the height of curve C. Also, the peak of the curve C does not coincide with the point f_1^a (figure 1c) where half of the nodes get connected, rather it has shifted to its right (unlike the ER case). The reason behind this is that even beyond the point f_1^a , smaller clusters keep getting formed and the decrease in the number of clusters (implying the merging of components) only begins at a larger value of f .

A cluster of k nodes connected cyclically with k edges is termed a k -cycle, and these emerge at $f \sim O(1/n)$ [16]. This remains true in Achlioptas networks even at this low n (figure 2c, dotted curve). At small f the tendency for the formation of k -cycles is more for Achlioptas networks (compared to ER) and the reverse is true for larger f . The origin of this effect can be traced to the relative frequency of the three components of the PR_m rule, the latter two options are significant only near the formation of the giant component [19].

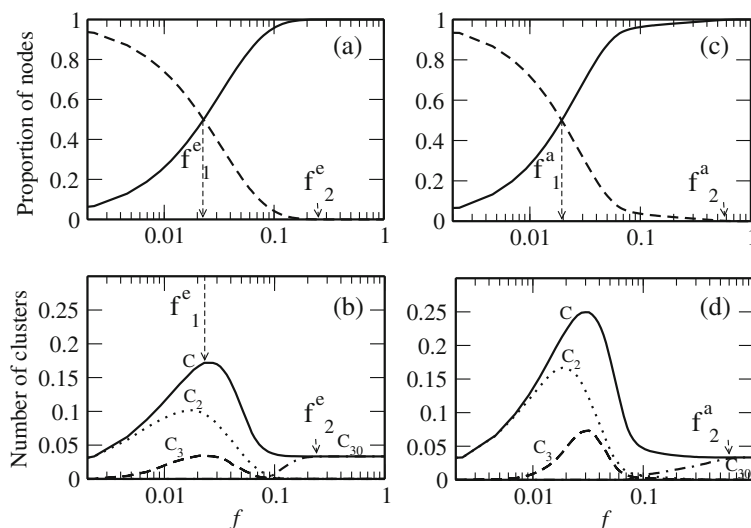


Figure 1. Structural features of the network as a function of f : (a) and (b) for ER, (c) and (d) for PR_m graphs. The solid (dashed) curves in (a) and (c) show the fraction of nodes in the network which (do not) have an edge. (b) and (d) Growth in the number of clusters of different sizes normalized by n (C_2 dotted, C_3 dashed and C_{30} with dots and dashes). The solid curve C shows the total number of clusters which is also normalized by n . The values for f_1^e , f_2^e , f_1^a and f_2^a are described in the text.

3. Excitable nodes

Each node of the random graph is occupied by a finite state cellular automaton that aims to model excitable dynamics. Each node can be active, silent, or refractory, corresponding to positive, zero or negative integer values for the variable [15]. Nodes are denoted $(r : b)$ where r is the total number of states allowed and b is the number of active states. So, there are $(r - b - 1)$ possible refractory states in addition to the single silent state. Thus, the state at node i denoted σ_i , takes values in $\{-(r - b - 1), -(r - b - 2), \dots, -1, 0, 1, 2, \dots, b\}$.

Excitable nodes can be classified into two types depending on the intrinsic time-scale of active and inactive stages. If $r > 2b$, nodes spend greater amount of time in the inactive states than in the active states in a complete cycle, while the reverse is true if $r \leq 2b$.

Given a configuration of the system at time t , the evolution proceeds as follows. When $\sigma_i(t) = 0$, $\sigma_i(t + 1) \rightarrow 1$ depending on the states of the nodes in the neighbourhood. If the node is in a refractory or active state, the value of the variable increases by 1 at each step,

$$\sigma_i(t + 1) = \sigma_i(t) + 1 \quad \text{if} \begin{cases} 1 \leq \sigma_i(t) \leq b - 1 \text{ or} \\ -(r - b - 1) \leq \sigma_i(t) < 0 \end{cases} \quad (1)$$

Once $\sigma_i(t)$ reaches the highest active state b , then it goes to the lowest refractory state, namely

$$\sigma_i(t + 1) = -(r - b - 1) \quad \text{if} \quad \sigma_i(t) = b, \quad (2)$$

and in the consequent time steps, $\sigma_i(t)$ increases by one till it reaches the silent state.

The manner in which the silent state turns into an active state is termed the loading rule [15] and this typically depends on the number of active and inactive neighbours $N_a(t)$ and $N_i(t)$ respectively, that a node has. Of the many possible loading rules, we consider two here.

In simple loading (SL) a silent state node switches to the active state provided it has at least one active neighbour,

$$\sigma_i(t + 1) = 1 \quad \text{if} \quad N_a(t) \geq 1. \quad (3)$$

In the majority rule (MR) a silent state switches provided a majority of its neighbours are active, namely

$$\sigma_i(t + 1) = 1 \quad \text{if} \quad N_a(t) \geq N_i(t). \quad (4)$$

In the next section we study the dynamics of 3:1 and 4:2 nodes on ER and Achlioptas random networks.

4. Interplay between structure and dynamics

A state of the network of n nodes is given by the n -vector

$$\vec{\sigma}(t) = \{\sigma_1(t), \sigma_2(t), \dots, \sigma_n(t)\} \quad (5)$$

which evolves, by the rules discussed above, to the state $\sigma(t + 1)$, and with time defines a trajectory in the phase space of dimension r^n . Since the phase space is finite, all trajectories must converge to an attractor which is either periodic with period p ,

$$\vec{\sigma}(t) = \vec{\sigma}(t + p) \quad (6)$$

or the unique fixed point [15],

$$\vec{\sigma}(t) \equiv 0. \tag{7}$$

which is stable.

We generate 2000 different random graphs with given f at fixed n , and for each choose 10,000 random initial conditions $\vec{\sigma}(0)$ to obtain the ensemble averaged steady state response of the network. A quantity that measures the dynamical activity is the fraction of initial conditions A_f that tend to a periodic solution [15], and this is evaluated for different loading rules on the two different random networks.

4.1 $r > 2b$ nodes

A network of 3:1 nodes has a state space of size 3^n . Under simple loading, any network can support a periodic solution if it contains a k -cycle ($k \geq 3$), and so the threshold for periodic solutions coincides with the threshold for the emergence of k cycles [15] for both the graphs as shown in figures 2a and c.

Next, we consider the majority loading rule (eq. (4)). The nature of activity observed in this scenario is fundamentally different from that observed in the SL case [15] (figures 2b and d). Here, very few initial states converge to a sustained activity pattern. Periodic solutions found in this case are the ones which live on minimal k -cycles, namely those where each node has degree 2. While the qualitative behaviour observed for both graphs is similar, the activity level of Achlioptas graphs is higher than on ER networks. With increasing f , though, the ER mechanism tends to reduce minimal cycles, while the Achlioptas process suppresses the addition of new nodes to clusters or cycles, thereby preserving them.

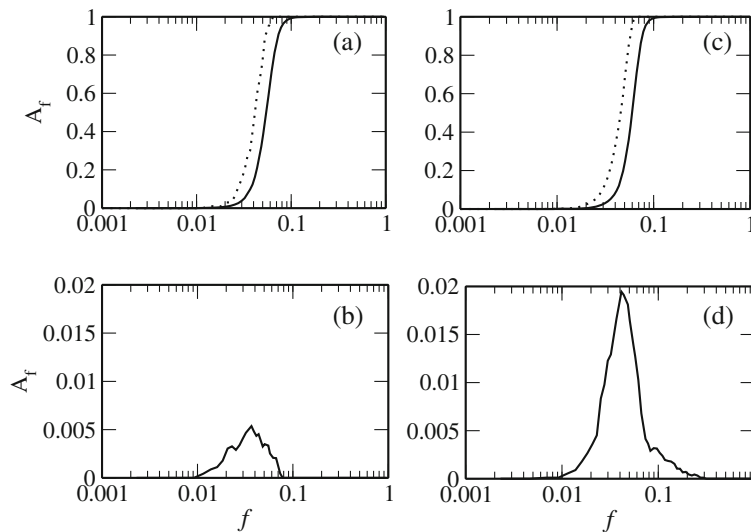


Figure 2. Activity curves of 3:1 nodes for the ER and PR_m graphs. (a), (c) Monotonic dynamics under SL (solid curve) emerges at the same threshold for the emergence of k -cycles (dashed curve). (b), (d) Dynamics under MR has a non-monotonic dependence on f .

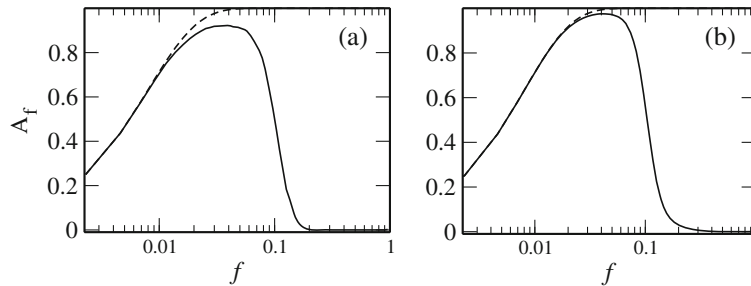


Figure 3. Activity curves for 4:2 nodes for the (a) ER and (b) PR_m networks. The solid (dashed) curve is the activity curve for nodes under MR (SL) loading rule. Prior to the local maximum for both graphs, the activity curves under the different loading rules are identical.

For different r and b , although the time-scales and thresholds will change depending on the specific loading rules that are applied, the dynamics tends to be qualitatively similar to the 3:1 case.

4.2 $r \leq 2b$ nodes

For $r \leq 2b$ node single edges suffice in supporting sustained dynamical activity: minimal k -cycles are not essential [15]. We consider networks of 4:2 nodes here as a representative example, however, in the large n limit the choice of r and b becomes very important in deciding the nature of dynamics [15].

Figure 3 gives a plot of A_f vs. f for the two networks with the different loading rules. Here also the majority rule results in a higher activity level for the Achlioptas network largely due to the maintenance of smaller structures over a larger range of f .

5. Summary

In the present paper we have investigated the interplay of network architecture and coupling in determining the dynamics of an automaton model on random graphs. These automata share many characteristics of neuronal systems – in particular, they have active, refractory and silent stages, and are coupled to each other through realistic mechanisms.

The manner in which the network is generated plays some role in determining the threshold for different dynamical phenomena. The two growth mechanisms studied here – ER and PR_m – belong to different universality classes [20]. The selection constraint that favours explosive percolation [18] also promotes the formation of pairs and triples of linked nodes while suppressing the merging of clusters over a larger range of connectivity. This has the effect of increasing the level of dynamical activity supported on the network and altering the thresholds for the emergence of some structural features in the random graphs. Some instances of such kinetic growth processes in physical systems are known [21], and thus it would be interesting to examine whether such examples also occur in extended excitable systems.

Acknowledgements

KM and TUS are Senior Research Fellows of the UGC and CSIR, India respectively. The authors thank Amit Bose for numerous discussions and generous advice.

References

- [1] D Terman and D Wang, *Physica* **D81**, 148 (1995)
- [2] D Yang, Y Li and A Kuznetsov, *Chaos* **19**, 033115 (2009)
- [3] M E J Newman and J Park, *Phys. Rev.* **E68**, 036122 (2003)
- [4] J M Montoya, S L Pimm and R V Solé, *Nature* **442**, 259 (2006)
- [5] S Jain and S Krishna, *Proc. Natl Acad. Sci.* **98**, 543 (2001)
- [6] C Meisel and T Gross, *Phys. Rev.* **E80**, 061917 (2009)
- [7] L Glass, *Nature* **410**, 277 (2001)
- [8] J Gansert, J Golowasch and F Nadim, *J. Neurophysiol.* **98**, 3450 (2007)
- [9] M E J Newman, *Phys. Rev.* **E66**, 016128 (2002)
- [10] R P Satorras and A Vespignani, *Phys. Rev. Lett.* **86**, 3200 (2001)
- [11] D H Zanette and S Gil, *Physica* **D224**, 156 (2006)
- [12] J Balthrop, S Forrest, M E J Newman and M M Williamson, *Science* **304**, 527 (2004)
- [13] C Borgers and N Kopell, *Neural Comput.* **15**, 509 (2006)
- [14] D Eytan and S Marom, *J. Neurosci.* **26**, 8465 (2006)
- [15] T U Singh, K Manchanda, R Ramaswamy and A Bose, *SIAM J. Appl. Dyn. Syst.* (2011) (in press)
- [16] P Erdős and A Rényi, *Publ. Math. Inst. Hung. Acad. Sci.* **5**, 17 (1960)
- [17] A L Barabási and R Albert, *Science* **286**, 509 (1999)
- [18] D Achlioptas, R M D'Souza and J Spencer, *Science* **323**, 1453 (2009)
- [19] Y S Cho, J S Kim, J Park, B Kahng and D Kim, *Phys. Rev. Lett.* **103**, 135702 (2009)
- [20] R M Ziff, *Phys. Rev. Lett.* **103**, 045701 (2009)
- [21] C D Lorenz, R Haghgoie, C Kennebrew and R M Ziff, *Surf. Sci.* **517**, 75 (2002)